

# Time efficient and quantitative Sodium imaging at 7T using compressed sensing accelerated FID spectroscopic imaging

Jetse van Gorp<sup>1</sup>, Paul de Bruin<sup>2</sup>, and Peter Seevinck<sup>1</sup>

<sup>1</sup>Image Sciences Institute, University Medical Center Utrecht, Utrecht, Netherlands, <sup>2</sup>Department of Radiology, Leiden University Medical Center, Leiden, Zuid-Holland, Netherlands

**Purpose:** To develop a time-efficient, flexible and quantitative <sup>23</sup>Na MR imaging strategy facilitating high SNR TSC determination as well as detailed characterization of multi-exponential <sup>23</sup>Na signal decay.

**Introduction:** With the availability of clinical 7T MRI scanners sodium (<sup>23</sup>Na) MRI has gained popularity in recent years for imaging of the brain, kidney, heart and cartilage. Although the higher field strength increases signal-to-noise ratio (SNR), the relatively low <sup>23</sup>Na NMR sensitivity and <sup>23</sup>Na concentration *in vivo* requires the acquisition of up to 20 signal averages, making <sup>23</sup>Na imaging time-consuming. Furthermore, the short T<sub>2</sub> of <sup>23</sup>Na has led to the use of (ultra)short TE radial and spiral gradient echo imaging techniques with relatively long sampling times to increase efficiency, however, at the cost of image blurring and sensitivity to off-resonance. Depending on the application either the total sodium concentration (TSC) (brain)<sup>1</sup> or the T2 signal decay related to bound and unbound <sup>23</sup>Na (orthopedic investigations)<sup>2,3</sup> is determined. Accurate quantification of the short T<sub>2</sub> component requires the acquisition of multiple echoes in a short time interval, which can prove to be challenging. In this work a 3D FID spectroscopic imaging technique (SI) is exploited to increase the overall SNR by maximizing the ratio between the total sampling and acquisition time<sup>4</sup>. The data acquired in the sampling interval can be used for retrospective adaptation of the sampling bandwidth (and thus the SNR), while also enabling detailed signal decay characterization for multi-exponential T<sub>2</sub> parameter mapping to discern multiple <sup>23</sup>Na pools. To reduce total scan time a spherical k-space shutter and variable density undersampling is used for compressed sensing acceleration.

**Methods: Phantom setup:** A cylindrical phantom containing 2% agar and 125mM NaCl<sub>2</sub> was made containing 5 tubes with the following <sup>23</sup>Na concentration: 25, 50, 100,150,250 mM. *In vivo* experiment: A healthy 35-year old male was subjected to a MRI exam. The study was in accordance with the IRB. Around the knee 6 tubes were positioned; 2 series of 0.75, 150 and 300 mM <sup>23</sup>Na either in 2% agar or in water. **Pulse sequence and hardware:** Experiments were performed on a whole body 7T scanner (Philips, Best) using an in-house built <sup>23</sup>Na birdcage coil combined with 4 <sup>1</sup>H-strip lines fed from a quadrature input. A 3D purely phase encoded FID-SI sequence was implemented with full control over the 3D (variable density under-) sampling pattern to accommodate compressed sensing reconstruction. **Imaging parameters:** 3D FID-SI data was acquired using a block pulse and non-selective excitation to ensure the shortest possible TE. Phantom images were acquired with voxel sizes 4x4x5mm (6.8min) and 6x6x5mm (6.8min and 3.4min with 2x CS), 32x32x32 acquisition matrix, sampling BW 32kHz, 512 points, TR/TE=25/1.25 ms. *In vivo* knee images were acquired with 3x3x5mm voxel size (21.8 min,2xCS), 64x64x32 acquisition matrix, TR/TE=40/1.5 ms, 32kHz sampling, 1024 points. **CS reconstruction:** A non-linear conjugate gradient solver<sup>4</sup> was used to minimize  $\lambda_w ||\psi_w m||_1 + \lambda_{TV} TV(m)$ <sup>5</sup>. The original 2D regularizations were replaced with a 3D wavelet (Daubechies 6) L<sub>1</sub> norm regularization and a 3D total variation norm regularization ( $\lambda_{TV}$ ) to reconstruct 3D-FID-SI data with three undersampled dimensions. To reconstruct the total 4D matrix the CS reconstruction was repeated for all time points after resampling to the desired sampling BW.

**Results: Signal decay characterization:** The signal decay curves of the <sup>23</sup>Na dilution series in 2% agar obtained with 3D-FID-SI are shown in Fig. 1. The relatively high sampling bandwidth of 32 kHz introduced noise (Fig. 1 a,c), which can be reduced dramatically without changing the signal decay characteristics by using a sliding window approach to artificially sample the signal at 2kHz. Although the signal decay curves predominantly demonstrate a linear behavior on a log-linear scale (Fig. 1 b,d), at short TE the highest two concentrations slightly deviate from linearity, suggesting the presence of a small fraction of short T<sub>2</sub> components.

**TSC determination:** Fig. 2 demonstrates <sup>23</sup>Na images of a cross-section of the agar phantom, reconstructed at different sampling bandwidths (1, 2, 8 kHz) following complex averaging, as well as an image depicting the spectral peak signal obtained by fourier transforming the temporal dimension. Reducing the sampling bandwidth increased the SNR, as already shown in Fig. 1. Interestingly, the image presenting the spectral peak intensities has the highest SNR. In the spectral domain full benefit is taken of the fact that 512 data points for each k-space location were obtained during 16 ms, resulting in a 512 images, which all add to the SNR of the spectrum as long as T<sub>acq</sub> < 1.26T<sub>2</sub><sup>4</sup>. In other words, the ratio of the sampling time over the total acquisition time was between 0.4 and 0.8 (T<sub>sampling</sub>/TR), which is extremely high and can be regarded as a measure for SNR efficiency of the imaging sequence. Two calibration curves (Fig 3), generally necessary for TSC determination, were determined based on the initial magnitude (M<sub>0</sub>) of the 1000Hz image (blue) and on the spectral peak maxima (orange). The latter shows the highest correlation (R<sup>2</sup> = 0.99), and suggests to be better suited to quantify low concentrations. **Compressed sensing:** The use of a spherical shutter and variable density undersampling enabled 4-fold acceleration with only minor reduction of spatial resolution, as shown by Fig. 4a,b. **In vivo knee images:** Using 4-fold accelerated 3D-FID-SI high SNR images of the knee were obtained depicting spectral peak maxima at a nominal resolution of 3x3x5mm and matrix size of 64x64x32 in 22min, with the highest signal intensities found in patellar and femorotibial cartilage in accordance to literature<sup>3</sup>.

**Conclusion and Discussion:** 3D-FID-SI was demonstrated to be a time-efficient, flexible and quantitative <sup>23</sup>Na MR imaging strategy facilitating high SNR TSC determination as well as detailed characterization of the multi-exponential <sup>23</sup>Na signal decay, related to bound and unbound sodium, if present. The method is perfectly suited for compressed sensing acceleration due to the fact that the 3D sampling pattern can be chosen freely. The absence of a readout gradient makes the method insensitive to B<sub>0</sub> related geometrical distortions, caused for example by imperfect shimming, the presence of air cavities in the brain or orthopedic metal objects. In order to confirm the added value of the method in clinical practice, future work should focus on quantitative comparisons to validate the accuracy of both TSC determination as well as multi-exponential signal characterization using short and long T<sub>2</sub> parameter mapping.

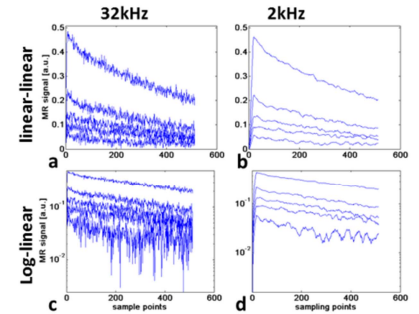


Fig. 1. Signal decay curves for the different <sup>23</sup>Na concentrations (top-down = 250,150,100,50,25 mM)

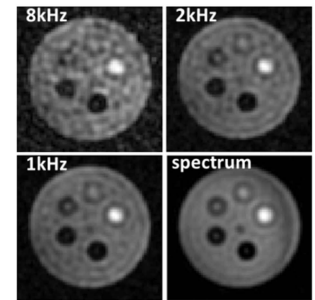


Fig. 2. Cross-sections of the phantom reconstructed at different BW (a-c) or representing the spectral signal (d).

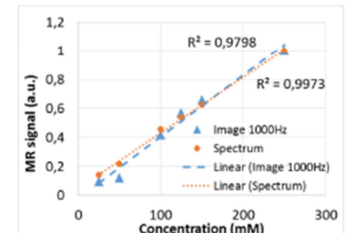


Fig. 3. MR signal as function of Na concentration

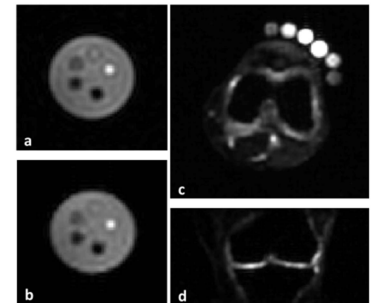


Fig. 4. CS reconstructed (b, c, d) and conventional reconstructed images. CS reconstructions were 4-fold accelerated with respect to fully sampled data.

References: 1. Mirkes, Magn. Reson. Med. DOI: 10.1002/mrm.25096 (2014), 2. Qiann, Magn. Reson. Med. DOI: 10.1002/mrm.25393 (2014), 3. Madelin G, Radiology, 268 (2013), 4. Pohmann, Journal of Magn. Reson. 129 p145-160 (1997), 5. M. Lustig, Magn. Reson. Med. 58, p1182-1195 (2007)